Facing the Challenge of Estimating Human Brain White Matter Pathways

Adelino R. Ferreira da Silva
Dep.º de Eng.ª Electrotécnica, Faculdade de Ciências e Tecnologia, FCT, Universidade Nova de Lisboa, 2829-516 Caparica, Portugal

Keywords: High Angular Resolution Diffusion Imaging (HARDI), Fiber Tractography.

Abstract: Diffusion anisotropy has been used to characterize white matter neuronal pathways in the human brain, and infer global connectivity in the central nervous system. However, mapping complex fiber configurations in vivo remains a challenging task. We present a new methodology to reduce uncertainty in estimating the orientation of neuronal pathways in high angular resolution diffusion imaging (HARDI) reconstructions. The methodology relies on three main features. First, an optimized HARDI reconstruction technique based on the generalized q-sampling imaging approach is adopted. Second, directional statistics are used to estimate orientation distribution function (ODF) profile directions from data distributed on the unit sphere. Third, a modified streamline algorithm able to accommodate multiple fiber tracts and multiple orientations per voxel is used, to exploit the directional information gathered from estimated ODF profiles. The methodology has been tested on synthetic data simulations of crossing fibers and on a real data set.

1 INTRODUCTION

Diffusion tensor imaging (DTI) is a widely used method in clinical research that models the average diffusion properties of water molecules inside a voxel based on a Gaussian diffusion assumption. Diffusion anisotropy, derived by DTI, has been used to characterize white matter neuronal pathways in the human brain, and infer global connectivity in the central nervous system (Basser et al., 2000). White matter fiber tractography is commonly implemented using the principal diffusion direction of the DTI model (Mori and van Zijl, 2002). Popular fiber tracking approaches, such as the streamline tracking algorithm, uses the DTI model to extract the orientation dependence of the diffusion probability density function of water molecules, and reconstruct the orientation distribution function (ODF) of anisotropic tissues. However, the standard single-tensor DTI model is based on a Gaussian diffusion assumption, thus unable to resolve crossing and splitting of fiber bundles.

High angular resolution diffusion imaging (HARDI) techniques have been proposed in the literature to overcome the limitations of the DTI method, and enable detection of multiple ODF maxima per voxel (see (Lenglet et al., 2009) for a review). Several studies have shown that fiber tracking based on HARDI-based techniques is improved and less sensitive to noise errors compared to tensor based tracking (Descoteaux et al., 2009), (Polzehl and Tabelow, 2011). The application of these methods is based on the assumption that the principal directions extracted from the ODF can be interpreted as principal directions of the underlying fiber architecture. Typically, local maxima of the reconstructed ODF are located simply by selecting a large number of randomly sampled points on the sphere and searching within a fixed radius neighborhood (Descoteaux et al., 2009). Some more sophisticated heuristics built on this basic approach have been proposed. For instance, in (Jian et al., 2007), a Quasi-Newton method is used to refine the position of each local maximum. However, as shown in (Özarslan et al., 2006) and (Lenglet et al., 2009), the peaks of the ODF profiles identified by these methods do not necessarily match the orientations of the distinct fiber populations. Since uncertainty in tractography arises from uncertainty in estimating the directions of propagation, HARDI reconstructions can still be ambiguous and difficult to interpret in the presence of complex fiber tract configurations. To reduce uncertainty and increase robustness in HARDI reconstructions, one may increase the number of sampling directions, and use higher strengths of diffusion-sensitive gradients (b-

R. Ferreira da Silva A..
Facing the Challenge of Estimating Human Brain White Matter Pathways.
DOI: 10.5220/0004177207090714
In *Proceedings of the 4th International Joint Conference on Computational Intelligence* (SSCN-2012), pages 709-714
ISBN: 978-989-8565-33-4

values) to attain satisfactory angular resolution (Cho et al., 2008). Unfortunately, this solution is impractical in clinical applications. Increasing the number of sampling directions prolongs the scan time, making HARDI reconstructions susceptible to motion-induced errors (Jiang et al., 2002). Using high b-values in clinical scanners results in low signal-to-noise ratio (SNR) and substantial diffusion-induced signal decay (Kuo et al., 2008). Poor SNR affects the accuracy of ODF reconstruction, and increases fiber orientation uncertainty.

In this paper, we present a new methodology to reduce uncertainty in estimating the orientation of neuronal pathways in HARDI reconstructions. The methodology may be summarized in the following three aspects. First, an optimized HARDI reconstruction technique based on the generalized q-sampling imaging (GQI) approach (Yeh et al., 2010) is adopted. Second, directional statistics are used to estimate ODF profile directions from data distributed on the unit sphere. The method focus on clustering data on the unit sphere, where complexity arises from representing ODF profiles as directional data. Sampling densities on the hemisphere are used in ODF profile mapping. Third, a modified streamline algorithm able to accommodate multiple fiber tracts and multiple orientations per voxel is used to exploit the directional information gathered from estimated ODF profiles. By combining HARDI reconstruction and directional statistics in an integrated framework, the methodology is expected to support more accurate fiber ODF estimation for white matter fiber tractography than other more traditional approaches. The methodology has been tested on synthetic data simulations of crossing fibers and on a real data set. The implementation is integrated in a coherent framework based on the R language (R Development Core Team, 2010) with 3D OpenGL visualization capabilities.

2 HARDI RECONSTRUCTIONS

The generalized q-sampling imaging method proposed in (Yeh et al., 2010) is a HARDI approach to estimate the ODF directly from diffusion MR signals. The relation between the acquired diffusion weighted images $W(\mathbf{r},\mathbf{q})$ and the measured ODF $\psi_m(\mathbf{r},\hat{\mathbf{u}})$ is given by

$$\psi_m(\mathbf{r},\hat{\mathbf{u}}) = A_q L_\Delta \sum_{\mathbf{q}} W(\mathbf{r},\mathbf{q}) \mathrm{sinc}(2\pi L_\Delta \mathbf{q}\cdot\hat{\mathbf{u}}), \quad (1)$$

where $\mathbf{r}$ is the voxel coordinate, $\hat{\mathbf{u}}$ represents a radial spherical unit direction, $\mathbf{q}$ is the wave vector in q-space, L_Δ is the diffusion sampling length, and A_q is a constant area term. The wave vector is given by $\mathbf{q} = \gamma\delta\mathbf{G}/2\pi$, where γ is the nuclear gyromagnetic ratio, and $\mathbf{G}$ and δ are the strength and duration of the diffusion-encoding gradient, respectively.

Equation (1) is simple to interpret. The estimated ODF is synthesized from a series of sinc basis functions, weighted by $W(\mathbf{r},\mathbf{q})$. The shape of the basis functions is determined by the value of $|\mathbf{q}|L_\Delta$. A higher value of $|\mathbf{q}|L_\Delta$ represents a sharper contour, and vice versa. Moreover, (1) specifies an operational sampling scheme in q-space from which the ODF can be estimated. In particular, the number of basis functions used in (1) is not restricted by the shell (or grid) resolution used for MRI signal acquisition. The number of radial sampling directions can be adapted for the purposes of ODF estimation. Typically, sampling densities of $N = 81$ and $N = 321$ on the hemisphere are used in ODF profile mapping, corresponding to a third and seventh-order tessellation of the icosahedron, respectively. However, this specification is not imposed a priori by the acquisition resolution on the GQI reconstruction process.

The second main feature of the proposed methodology is concerned with multiple directional mapping. Starting with the raw HARDI signal acquired on a grid of q-space, the ODF profile is estimated at each voxel, considering a sampling density of unit vectors on a unit $\mathbb{S}2$ grid. When a threshold is applied to the estimated ODF at each voxel, the non-thresholded unit vectors provide directional statistics information about the estimated ODF profile. The main ODF orientations at each voxel relevant for fiber tracking may be estimated by clustering the non-thresholded unit vectors. This directional clustering procedure has several advantages compared to traditional approaches for orientation mapping. In fact, current best practices perform multiple maxima extraction based on procedures which are very sensitive to the local modes that appear in the reconstructed ODFs. Signal noise and low sampling resolution yield deformed ODF reconstruction profiles, thus affecting accuracy of the multiple orientation determination. In contrast, estimating orientations from clustered directional data is much less sensitive to local modes in the reconstructed ODF profile. Moreover, the procedure is more robust to noise since it estimates orientations statistically from sampled data.

For directional clustering estimation, we consider a mixture of k von Mises-Fisher (vMF) distributions (Banerjee et al., 2005) that serves as a model for directional ODF profile data, corresponding to multiple fiber orientations. A mixture of k vMF distributions has a density given by

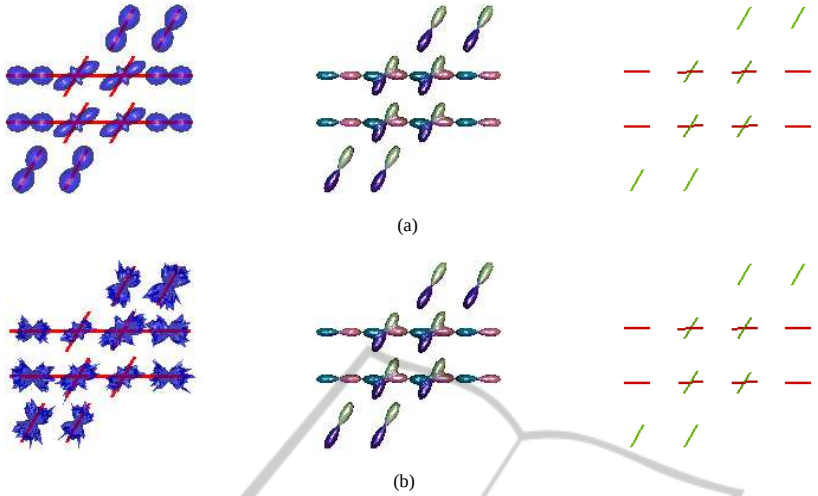

Figure 1: (a) Simulated noise free field of diffusion profiles, reconstructed field of ODF glyphs, and estimated ODF directions, from left-to-right respectively. (b) Simulation as in (a) with Rician noise level SNR=30.

$$f(x|\Theta) = \sum_{h=1}^{k} \alpha_h f_h(x|\theta_h), \qquad (2)$$

where $f_h(x|\theta_h)$ denotes a vMF distribution with parameter $\theta_h = (\mu_h, \kappa_h)$ for $1 \leq h \leq k$, $\Theta = \{\alpha_1, \ldots, \alpha_k, \theta_1, \ldots, \theta_k\}$, and the α_h are non-negative and sum to 1. A d-dimensional unit random vector $x \in \mathbb{S}^{d-1}$ is said to have d-variate vMF distribution if its probability density function is given by

$$f_h(x|\mu, \kappa) = c_d(\kappa) e^{\kappa \mu^T x}, \qquad (3)$$

where $\|\mu\| = 1$, $\kappa \geq 0$, $d \geq 2$, and $c_d(\kappa)$ is a normalizing constant (Mardia and Jupp, 2000). The density $f_h(x|\mu, \kappa)$ is parameterized by the mean direction μ, and the concentration parameter κ. The κ parameter characterizes how strongly the unit vectors drawn according to $f_h(x|\mu, \kappa)$ are concentrated about the mean direction μ. In this work, we used the procedure for clustering directional data outlined in (Banerjee et al., 2005), and implemented in (Hornik and Grün, 2011).

3 EXPERIMENTS

3.1 Simulated Field of Diffusion Profiles

To illustrate the methodology described in Section 2, we generated a field of simulated diffusion profiles as depicted in Figure 1. The field simulates crossing fibers with an angle of 60°, and b=4500. Figure 1(a) illustrates the simulated noise free field, the reconstructed field of ODF glyphs using the GQI method, and the estimated ODF directions based on the vMF mixture approach. A similar profile simulation with added Rician noise, and a signal-to-noise (SNR) value of 30 is shown in Figure 1(b). As illustrated, the vMF approach correctly identifies the underlying fiber orientations in both cases.

3.2 Real Data Experiment

We report on experiments using a DICOM data set provided by the "Advanced Biomedical MRI Lab, National Taiwan University Hospital". Specifically, we have used the data set "DSI 203-point 3mm" which is included in the "DSI Studio" package, publicly available from the NITRC repository (http://www.nitrc.org). This data set is from a normal 24-year-old male volunteer, and has been provided as a demonstration data set in connection with the "DSI Studio" software for diffusion MR images analysis (Yeh et al., 2010). The data set was obtained with an echo planar imaging diffusion sequence with twice-refocused echo, dimension $64 \times 64 \times 40$, and slice thickness 2.9 mm. Further details on the data set specification are available from the NITRC repository. We have tested our model with the two b-tables that accompanies the data set. One is a b-table for a $\mathbb{S}2$-like grid denoted by "dsi203_bmax4000.txt". The other is the b-table for the 3D-DSI sampling scheme used in the DICOM data acquisition. This b-table has 203 points uniformly distributed on a 3D grid limited to the volume of the unit sphere. In both tables, the b-values range from 0 to 4000.

Figure 2 shows the views sagittal, coronal and axial for slices $[X, Y, Z] = [22, 29, 24]$ of a region of interest (ROI) overlayed on the original data set with non-brain tissue removed. The ROI image depicts brain regions where anatomic white matter fiber crossings

Figure 2: Sagittal, coronal and axial views (from left-to-right) for slices $[X,Y,Z] = [22,29,24]$ of the selected ROI volume overlayed on the original data set with non-brain tissue removed. The sagittal view has the front brain facing right; coronal and axial views have the right hemisphere on the left of the image (radiological convention).

Figure 3: Linemaps for the field of profiles estimated from the ODFs, for voxels in axial slices 23 (left), and 24 (right). The panels also depict the ROI (SLF and CT regions as dark hues) overlayed on the central regions of slices 23 and 24.

are known to exist, forming multiple pathway bundles connected to the cerebral cortex. The ROI was formed by extracting the superior longitudinal fasciculus (SLF) and corticospinal tract (CT) regions based on the "ICBM-DTI-81 White-Matter" atlas included in the FSL toolbox (Smith et al., 2004). The extracted regions were registered to the DSI data set using the FSL/FLIRT tool. Using the procedure outlined in Section 2, we estimated for each voxel of the DSI data set the main ODF directions. This information enables us to draw linemaps showing the estimated orientations, and number of fibers for each voxel.

We show in Figure 3 linemaps for the field of profiles estimated from the ODFs, for voxels in axial slices 23 (left), and 24 (right). The selected ROI image is overlayed on Figure 3, in order to pinpoint the location of the SLF and CT regions on the linemaps. Figure 3 depicts central regions of slices 23 and 24, where a large number of voxels with crossing fibers is clearly visible (see right SLF for slice 23, and left SLF for slice 24). The central area in Figure 3 is typical of horizontal fibers associated with the corpus callosum.

Using the estimated voxel directional information, we implemented a streamline tractographic algorithm to represent and visualize the fiber tracts. The algorithm is a modified version of the fiber tracking algorithm described in (Mori and van Zijl, 2002). The modifications were implemented in order to deal with multiple directional orientations and multiple fiber tracts per voxel. Fiber tracts are initiated in every voxel within a specified user defined ROI using one of the estimated main voxel ODF directions, and are extended bi-directionally in steps less than half of the voxel dimension. The tracts are then propagated a step parallel to the selected direction. For each new voxel in the path front, one specific direction among the estimated voxel ODF directions is selected. The voxel ODF direction that produces least curvature with the incoming path is selected for propagation. Multiple tracts per voxel are accommodated by initializing the tracts with random real values within the seed voxel. The number of initializing tracts may be specified by the user, enabling him to strike a bal-

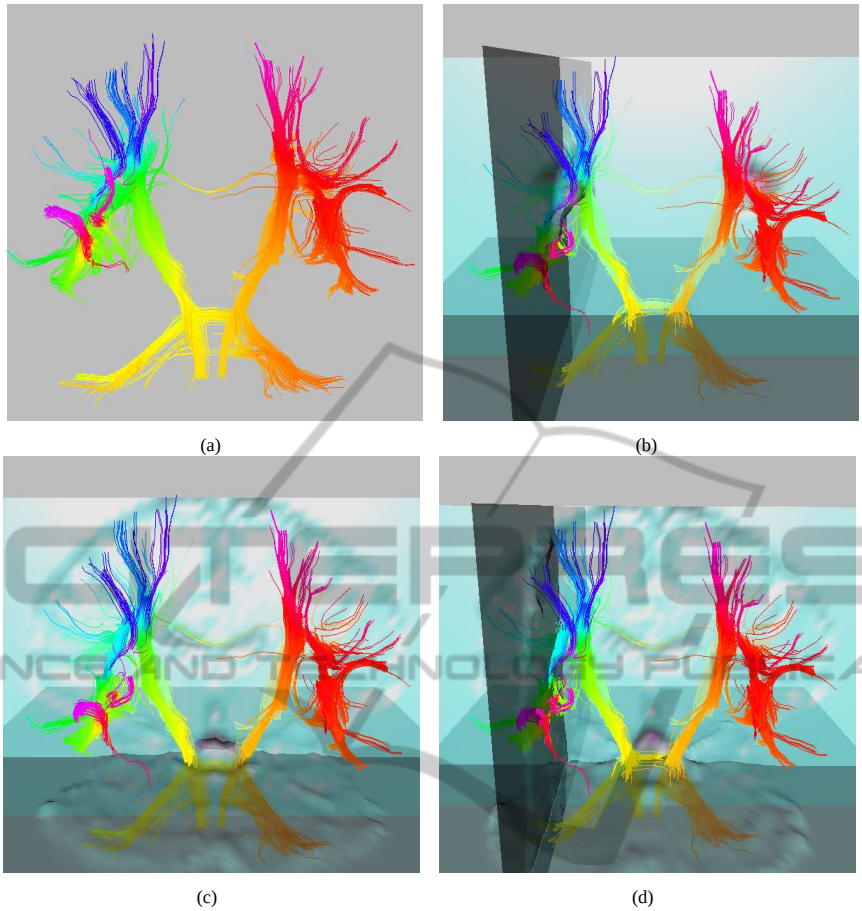

Figure 4: Panels representing the 3D OpenGL interface used to visualize the estimated fiber pattern in the context of the brain anatomy: (a) Estimated fiber pattern using multiple directional orientation and multiple fiber tracts per voxel; In (b) fiber tracts are overlayed on image slices of the selected ROI region; In (c) and (d) fiber tracts are overlayed on image slices of the brain.

ance between fiber bundle density and running time. The usual criteria for line keeping and line termination have been adopted. In particular, the following criteria have been specified: minimum fiber length (50 mm), maximum fiber length (600 mm), maximum admissible fiber deviation angle(60^o), and generalized fractional anisotropy threshold (0.2). In Figure 4 we show several panels representing the 3D OpenGL (Adler and Murdoch, 2010) interface used to visualize the estimated fiber pattern in the context of the brain anatomy. Figure 4(a) illustrates the pattern of interconnections using the voxels in SLF and CT regions as seeds, and bundles with 10 randomly initialized tracts per voxel. Figure 4(b) maps the fiber tracts overlayed on image slices of the selected ROI region. Figure 4(c) and Figure 4(d) map the fiber tracts overlayed on image slices of the brain.

4 CONCLUSIONS

We have presented a HARDI reconstruction approach incorporating directional statistics information to support in vivo fiber tractography. Based on experiments, the proposed approach was found to be more accurate in estimating local fiber orientations than traditional deterministic techniques based on multiple maxima extraction. Directional accuracy impacts strongly on the quality of the reconstructed fiber maps, and subsequent interpretation of fiber tract anatomy for use in clinical imaging. An extended tractographic procedure able to accommodate multiple pathways and bundled fibers was outlined to profit from the richer directional information gathered at each voxel.

The proposed approach applies statistical information criteria to decide on the number of components (voxel fibers) to select. The BIC selection criterion used for discriminating between single- and

crossing-fiber voxel configurations, as well as for estimating the number of fibers per voxel, was adequate. Nevertheless, one drawback of the proposed methodology concerns the necessity of applying model selection criteria to estimate the number of components in the mixture. For multiple fiber profiles, the fitting process has to be applied repeatedly to different configurations before the best final decision is estimated. This algorithmic process entails higher time-complexities than deterministic ones.

We believe that the directional statistics technique proposed in this work offers significant increases in sensitivity for anatomical analysis over traditional approaches. We intend to build on the quantitative and qualitative information provided by the proposed directional statistics approach to support the study of fiber tract architecture in the brain. In particular, this information may be explored to build robust probabilistic tractographic algorithms for complex fiber configurations.

REFERENCES

Adler, D. and Murdoch, D. (2010). *rgl: 3D Visualization Device System (OpenGL)*. R package version 0.92.879.

Banerjee, A., Dhillon, I. S., Ghosh, J., and Sra, S. (2005). Clustering on the Unit Hypersphere using von Mises-Fisher Distributions. *Journal of Machine Learning Research*, 6:1345–1382.

Basser, P. J., Pajevic, S., Pierpaoli, C., Duda, J., and Aldroubi, A. (2000). In Vivo Fiber Tractography Using DT-MRI Data. *Magnetic Resonance in Medicine*, 44:625–632.

Cho, K.-H., Yeh, C.-H., Tournier, J.-D., Chao, Y.-P., Chen, J.-H., and Lin, C.-P. (2008). Evaluation of the accuracy and angular resolution of q-ball imaging. *NeuroImage*, 42:262–271.

Descoteaux, M., Deriche, R., Knösch, T. R., and Anwander, A. (2009). Deterministic and Probabilistic Tractography Based on Complex Fibre Orientation Distributions. *IEEE Transactions on Medical Imaging*, 28(2):269–286.

Hornik, K. and Grün, B. (2011). *Mixtures of von Mises Fisher Distributions*. R package version 0.0-0.

Jian, B., Vemuri, B. C., Özarslan, E., Carney, P. R., and Mareci, T. H. (2007). A novel tensor distribution model for the diffusion-weighted MR signal. *NeuroImage*, 37:164–176.

Jiang, H., Golay, X., van Zijl, P. C., and Mori, S. (2002). Origin and minimization of residual motion-related artifacts in navigator-corrected segmented diffusion-weighted EPI of the human brain. *Magnetic Resonance in Medicine*, 47:818–822.

Kuo, L.-W., Chen, J.-H., Wedeen, V. J., and Tseng, W.-Y. I. (2008). Optimization of diffusion spectrum imaging and q-ball imaging on clinical MRI system. *NeuroImage*, 41:7–18.

Lenglet, C., Campbell, J. S. W., Descoteaux, M., Haro, G., Savadjiev, P., Wassermann, D., Anwander, A., Deriche, R., Pike, G. B., Sapiro, G., Siddiqi, K., and Thompson, P. M. (2009). Mathematical methods for diffusion MRI processing. *NeuroImage*, 45(1, Supplement 1):S111–S122.

Mardia, K. V. and Jupp, P. (2000). *Directional Statistics*. John Wiley and Sons Ltd., 2nd edition.

Mori, S. and van Zijl, P. C. M. (2002). Fiber tracking: principles and strategies - a technical review. *NMR in Biomedicine*, 15:468–480.

Özarslan, E., Shepherd, T. M., Vemuri, B. C., Blackband, S. J., and Mareci, T. H. (2006). Resolution of complex tissue microarchitecture using the diffusion orientation transform (DOT). *NeuroImage*, 31:1086–1103.

Polzehl, J. and Tabelow, K. (2011). dti: Beyond the Gaussian Model in Diffusion-Weighted Imaging. *Journal of Statistical Software*, 44(12).

R Development Core Team (2010). *R: A Language and Environment for Statistical Computing*. R Foundation for Statistical Computing, Vienna, Austria.

Smith, S. M., Jenkinson, M., Woolrich, M. W., Beckmann, C. F., Behrens, T. E. J., Johansen-Berg, H., Bannister, P. R., Luca, M. D., Drobnjak, I., Flitney, D. E., Niazy, R. K., Saunders, J., Vickers, J., Zhang, Y., Stefano, N. D., Brad, J. M., and Matthews, P. M. (2004). Advances in Functional and Structural MR Image Analysis and Implementation as FSL. Technical Report TR04SS2, FMRIB (Oxford Centre for Functional Magnetic Resonance Imaging of the Brain).

Yeh, F.-C., Wedeen, V. J., and Tseng, W.-Y. I. (2010). Generalized q-Sampling Imaging. *IEEE Transactions on Medical Imaging*, 29(9):1626–1635.